

Supporting Information

Revisiting the dissolution-recrystallization mechanism of rutile growth from protonated titanate nanotubes

Yanxin Chen^a, Fan Wu^a, Lijing Fan^a, Shaohua Chen^a, Jieyi Shen^a, Pengxin Liu^{a,b,*}

^a School of Physical Science and Technology, ShanghaiTech University, Shanghai 201210, People's Republic of China

^b Shanghai Key Laboratory of High-Resolution Electron Microscopy, ShanghaiTech University, Shanghai 201210, People's Republic of China

*Email: liupx@shanghaitech.edu.cn

The PDF file includes:

Materials and Methods

Figures. S1 to S28

Table S1

References

Materials and Methods

1. Chemicals and Materials

Sodium hydroxide (NaOH), hydrochloric acid (HCl 36%) and ethanol were purchased from Sinopharm Chemical Reagent Co., Ltd. (Shanghai, China). Anatase was purchased from Adamas. Aeroxide TiO₂ P25 was purchased from Evonik. All chemicals were used as received without further purifications. The water used in all experiments was ultrapure (18.2 MΩ) purified using HHitech Master touch-Q15 Laboratory Water Purification System.

2. Characterization methods

Transmission electron microscopy (TEM), high-resolution TEM (HRTEM) and selected-area electron diffraction (SAED) results were collected on a JEOL F200 transmission electron microscope operating at 200 kV. For the preparation of powder samples, rutile and protonated titanate samples were dispersed in 50 mL ethanol for sampling onto the copper grid. For time-tracking experiments, the samples of supernatant were diluted by 50 mL ethanol. The solution was casted onto 300-mesh carbon coated copper grid through impregnation. The sampling process was repeated 5 times when the ethanol evaporated completely each time.

N₂ adsorption-desorption isotherms (BET) at 77 K were collected from a Quantachrome Autosorb-iQ-MP AG using liquid N₂ Dewar for temperature control. The samples were degassed at 120 °C under vacuum for 12 h before measurement.

Powder X-ray diffraction (PXRD) patterns were recorded on Bruker D2 instrument

with Cu K α radiation ($\lambda = 1.5418 \text{ \AA}$) under 30 kV and 10 mA. Optics Primary Motorized Slit was 1 mm. PSD opening was 2.93395°. The scanning rate was 0.2°/s from 5° to 90°.

X-band electron-paramagnetic resonance (EPR) spectra were recorded using a Bruker electron spin resonance spectrometer (ESR 5000). Measurements were conducted at room temperature and 30 mW.

UV-Vis diffuse reflection spectroscopy (UV-Vis DRS) was conducted on Agilent Cary 5000 UV with an integrating sphere. The scanning rate was 600 nm/min from 800 nm to 200 nm.

Thermogravimetric analysis (TGA) and differential scanning calorimetric (DSC) analysis was carried out on Mettler Toledo TGA/DSC 3+ with a heating rate of 5 °C /min from 30 °C to 800 °C in synthetic air flow (50 mL/min). The sample was loaded into a 70 μ L alumina crucible. For protonated titanate, the sample was ground into powder and filled into the crucible.

Raman spectra were recorded on Renishaw Invia (UK) confocal Raman microscope equipped with 532 nm lasers. The object lens with a numerical aperture of 0.55 was used in the system. Spot diameter was 1.2 μ m at the power of 3.32 mW.

Dynamic light scattering (DLS) measurements were carried out on an Anton Paar Litesizer 500 Particle Analyzer at an angle of 175° with a 658 nm laser. About 1 mL solution for each sample was loaded into a disposable measurement cuvette. DI water was used as the solvent whose refractive index is 1.4331 and viscosity is 13.0444 mPa·s, for calculations.

3. Mass Quantification

According to the TGA results (Figure S5), dried PTN still contained 27 w% water. The quantification of all samples based on weighing need to consider the water content. One method is to base on the mole of Ti, considering all samples turn into pure titanium dioxide upon calcination. Hence, the end point of TGA measurements should be able to provide the exact quantity of Ti.

Take the feed amount as an example, for 0.1 M concentration of Ti in each 10 mL acid solution, 0.11 g PTN was feed. The quantification method is as follows.

$$\begin{aligned}n_{Ti} &= cV = 0.1 \text{ mol/L} \times 0.01 \text{ L} = 0.001 \text{ mol}; \\m_{TiO_2} &= 0.001 \text{ mol} \times 79.87 \text{ g/mol} = 0.07987 \text{ g}; \\m_{PTN} &= m_{TiO_2} \div 73\% \approx 0.1094 \text{ g}\end{aligned}$$

Supporting Figures

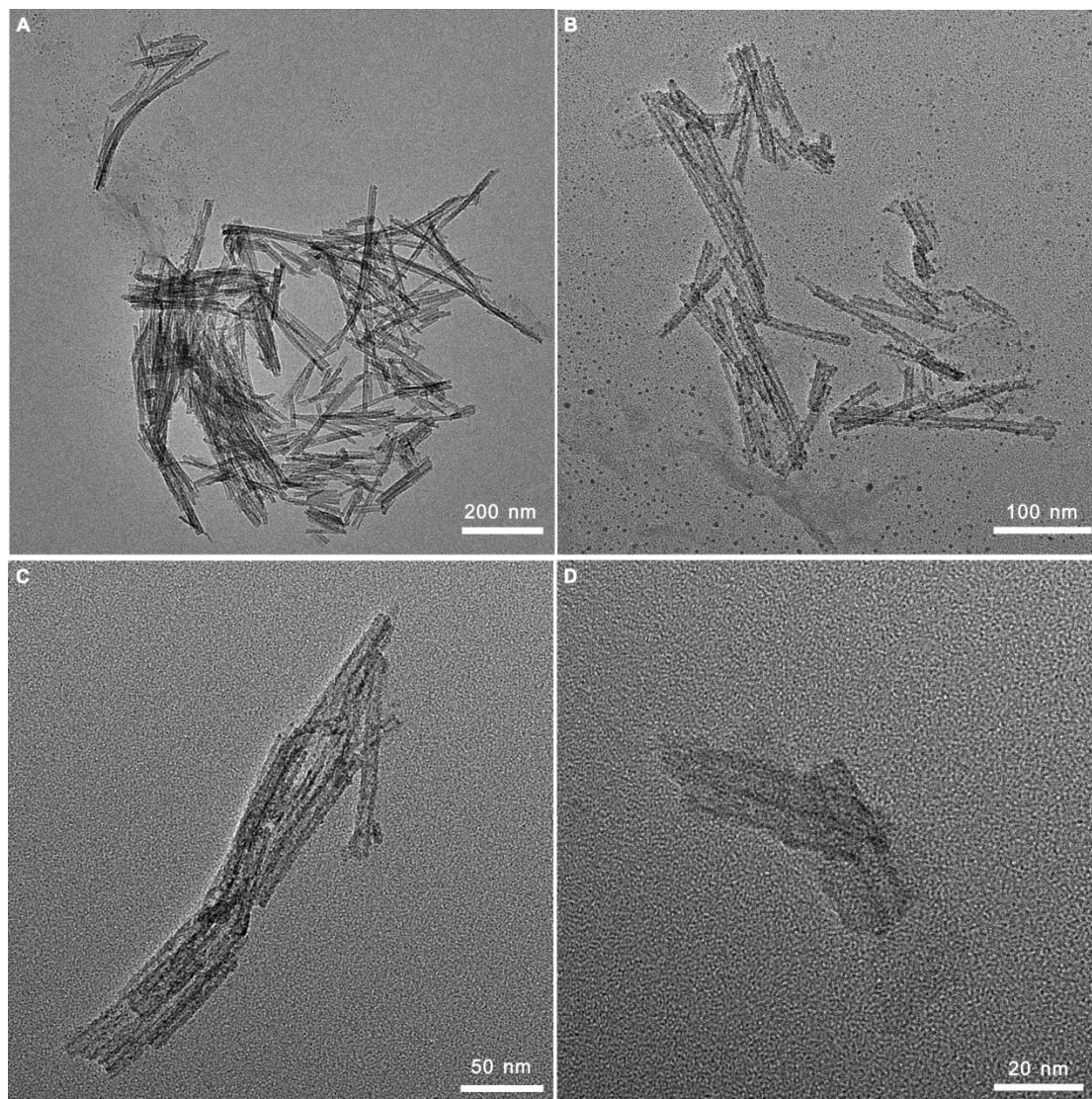


Figure S1. Representative TEM images of protonated titanate nanotubes (PTN).

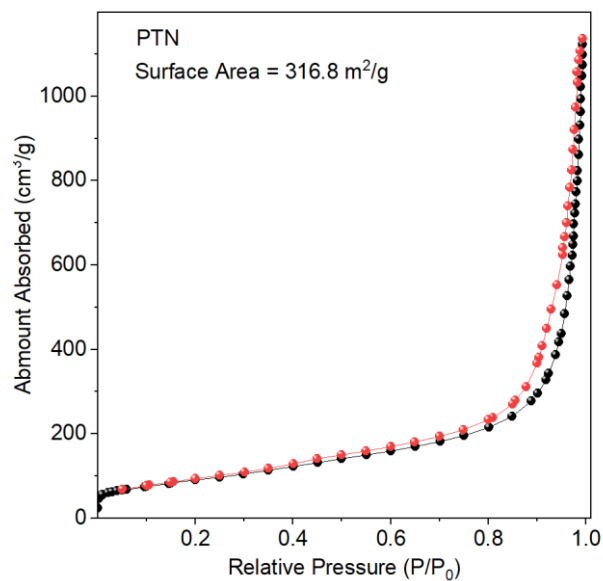


Figure S2. N₂ adsorption-desorption isotherms of PTN. The isotherms showed a typical type IV hysteresis loop, which was consistent with the tubular morphologies.

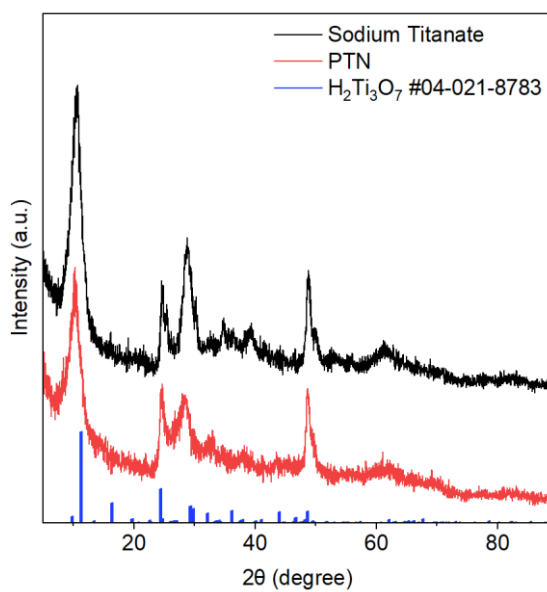


Figure S3. pXRD patterns of sodium titanate and PTN resembled those of layered titanates.^[1]

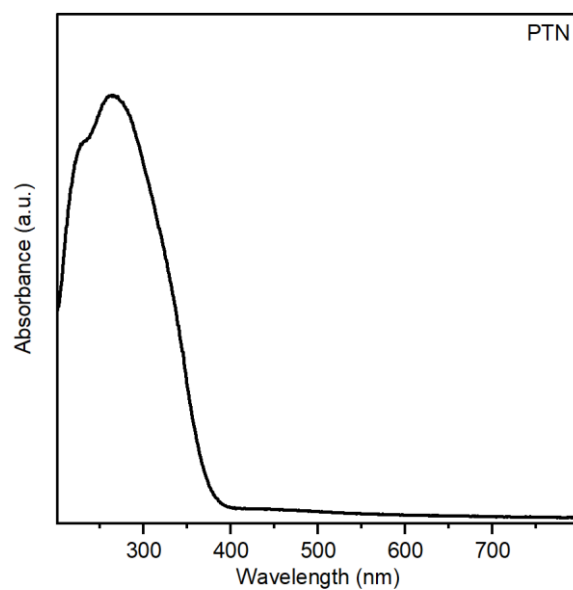


Figure S4. UV-vis DRS of PTN.

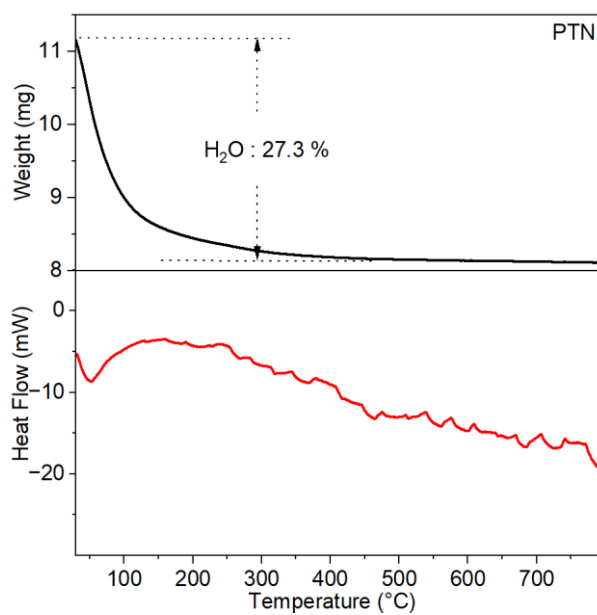


Figure S5. TGA and DSC curves of PTN. The 27.3 % weight loss from 50 °C to 460 °C was assigned to physically adsorbed water and released water upon decomposition.

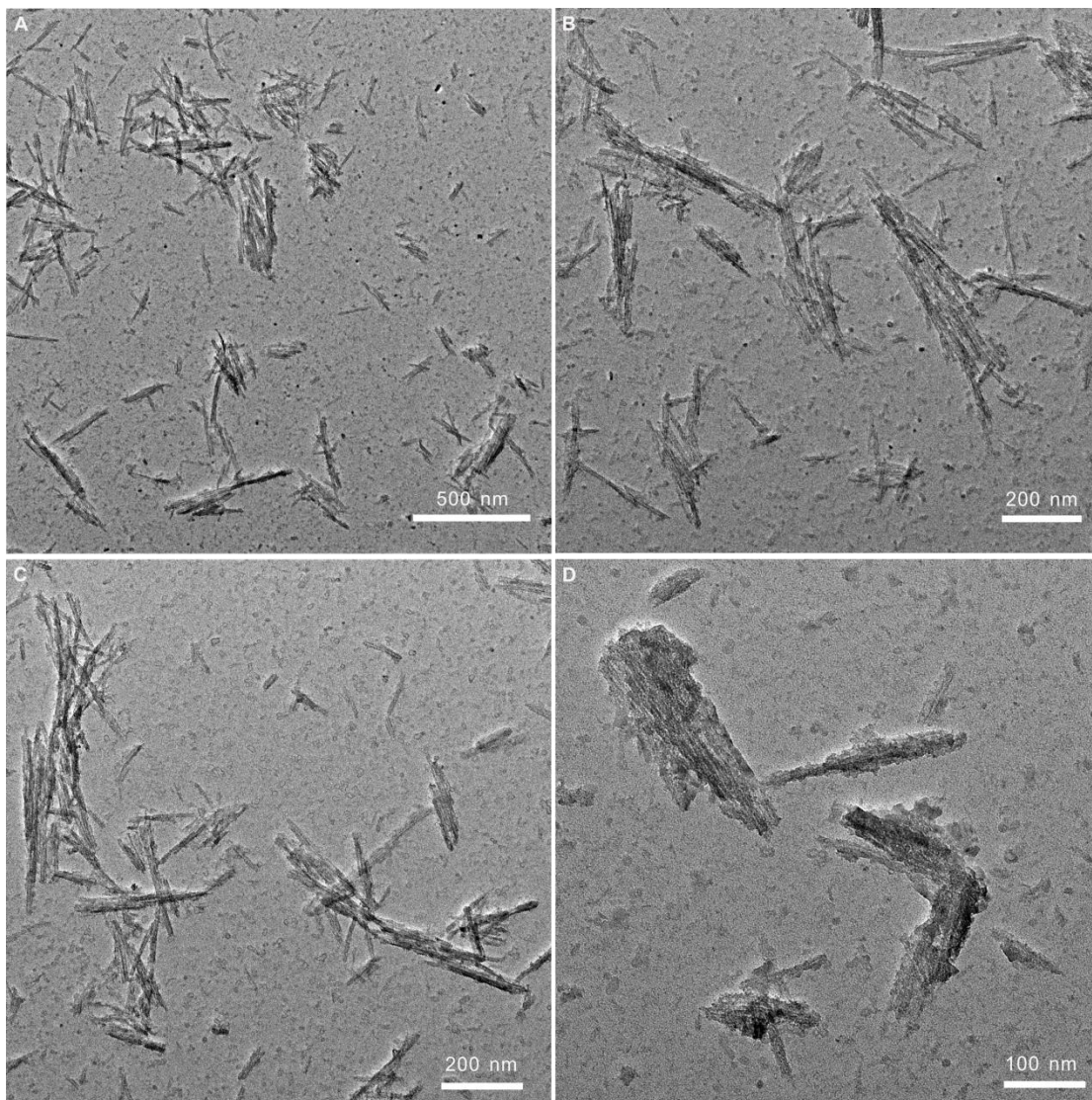


Figure S6. Representative TEM images of the solid residue after dispersing PTN in 3 M HCl for 2 hours.

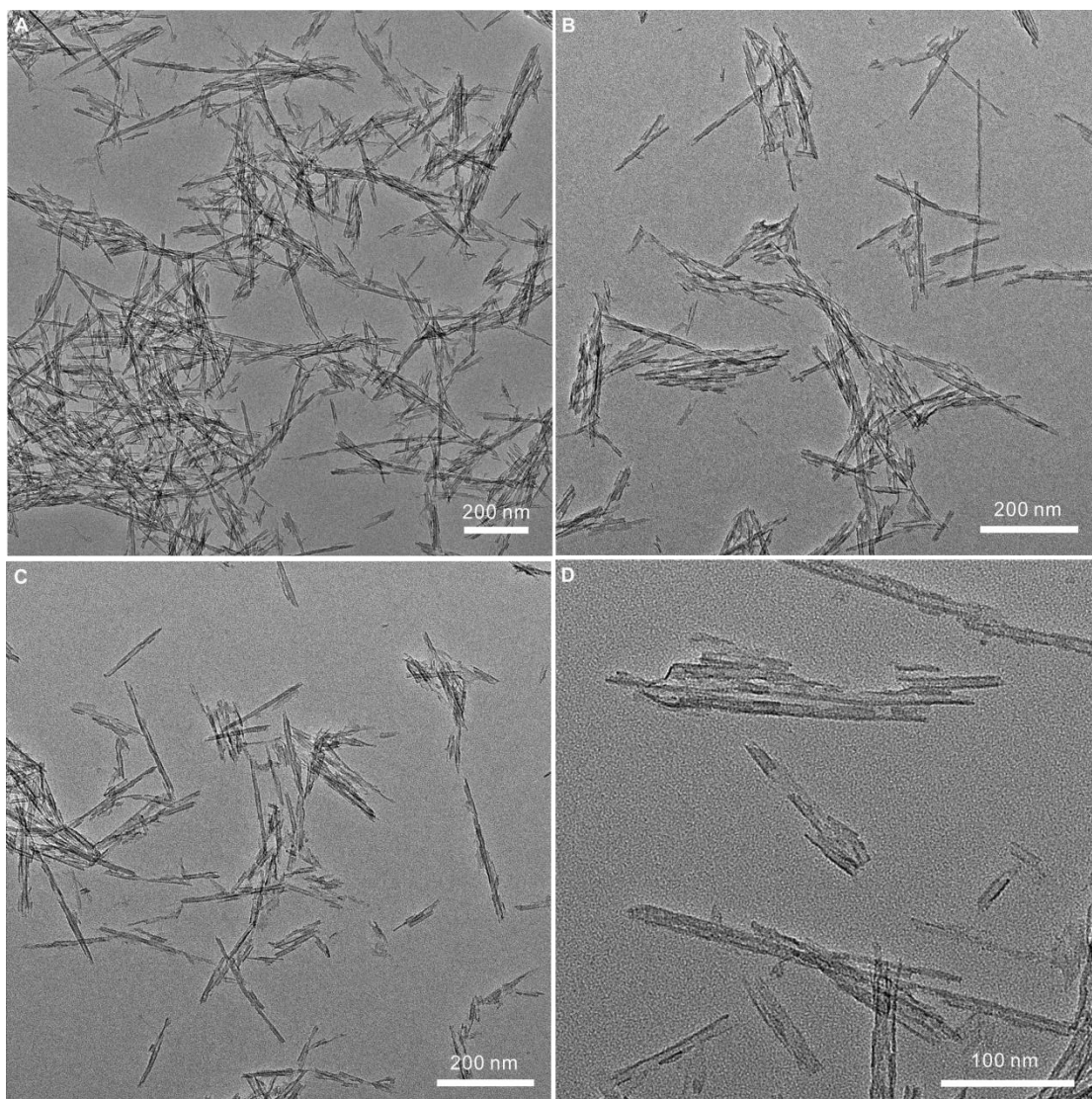


Figure S7. Representative TEM images of the solid residue after dispersing PTN in 3 M HCl for 5 hours.

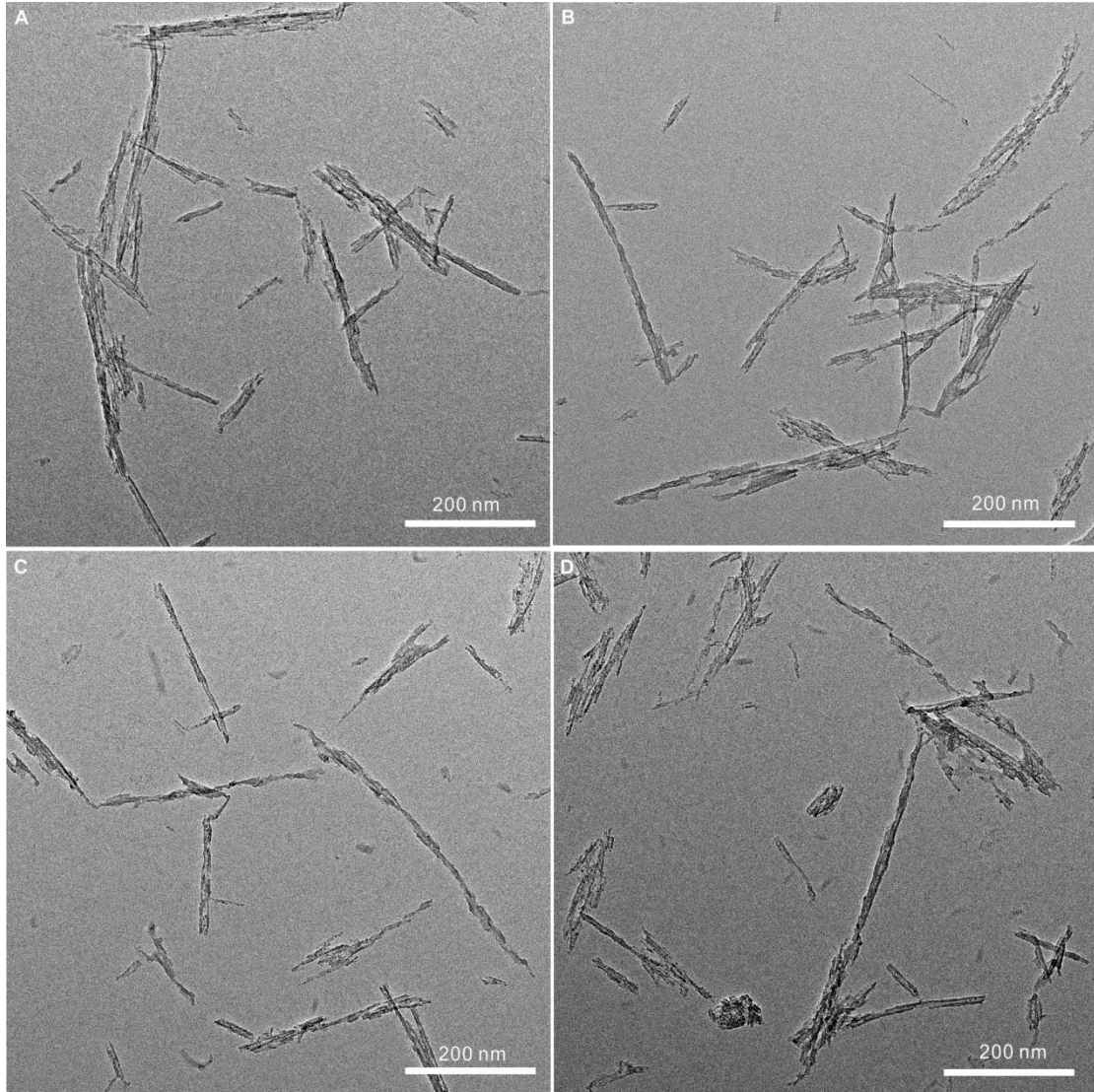


Figure S8. Representative TEM images of the solid residue after dispersing PTN in 3 M HCl for 12 hours.

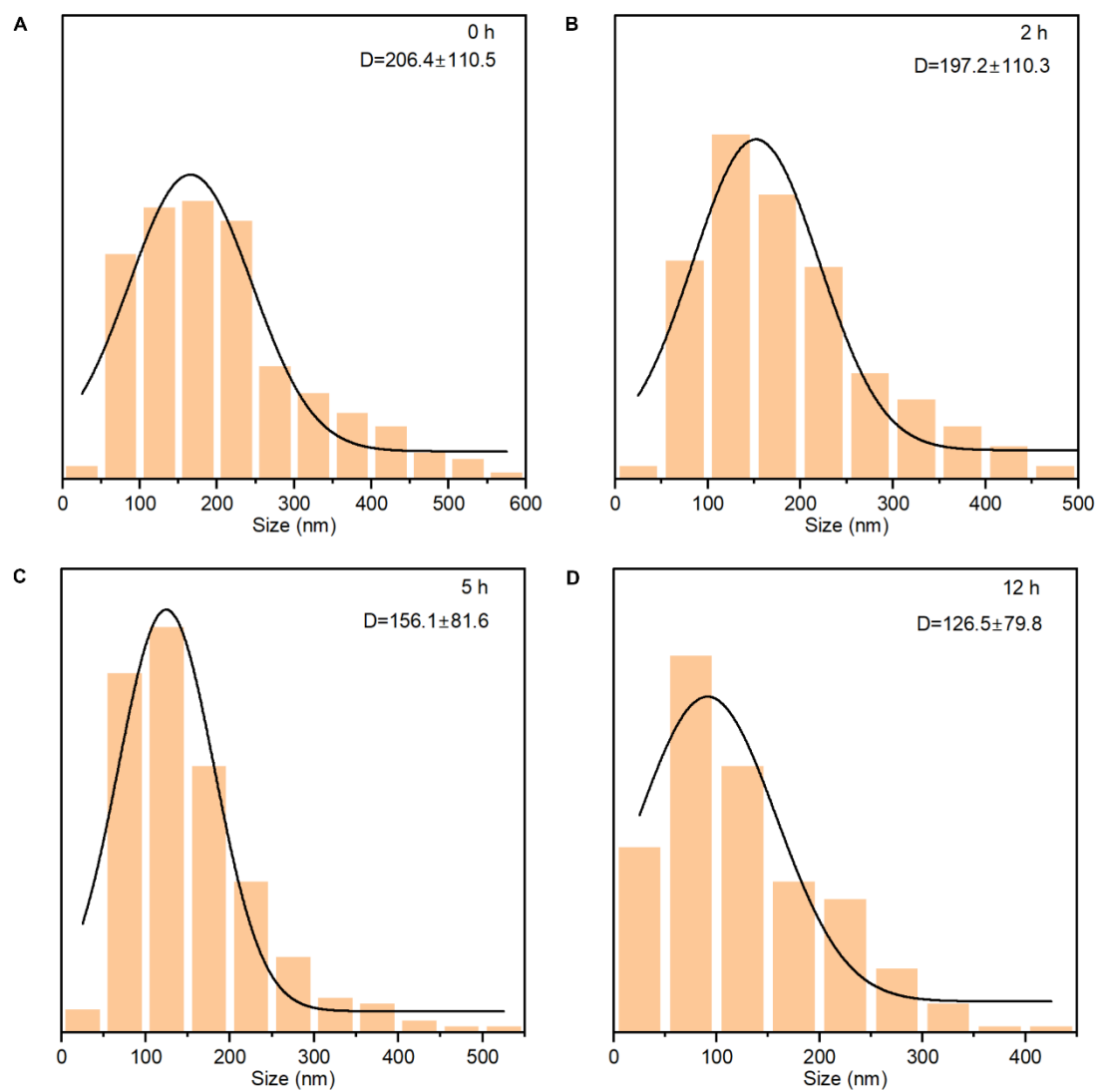


Figure S9. Particle size distribution statistics based on TEM images.

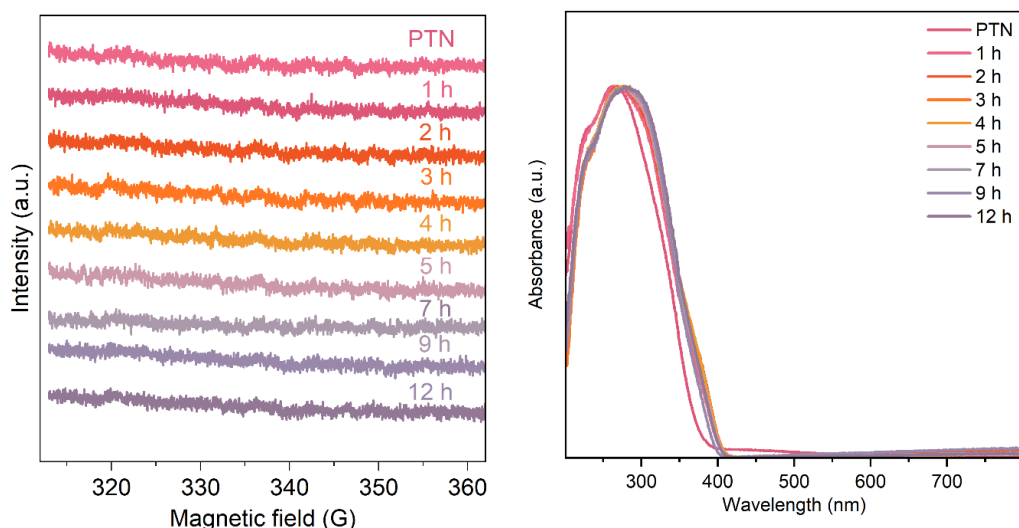


Figure S10. EPR (left) and UV-vis DRS (right) of undissolved PTN sampled after different durations of mixing PTN with acid. Reaction condition: 0.1 M Ti in 3 M HCl. The small shift between PTN and other intermediate samples was likely due to the destruction of the nanotube structure during the dissolution process.

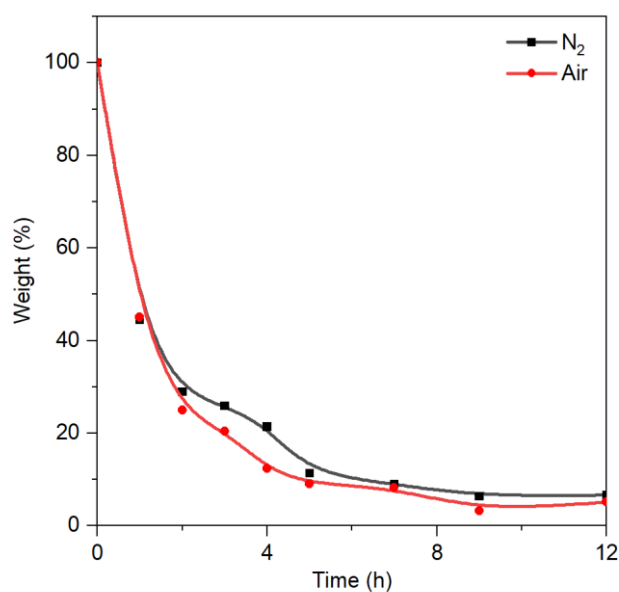


Figure S11. Time-tracking experiments on the dissolution of PTN in 3 M HCl by measuring the weight of the solid residue. The reactions were operated either under air atmosphere or N₂ atmosphere. Reaction condition: 0.1 M Ti in 3 M HCl. For N₂ experiment, the dispersion was placed in a three-necked flask and purged with nitrogen overnight. During the sampling process, the nitrogen atmosphere was kept to maintain an oxygen-free environment in the system.

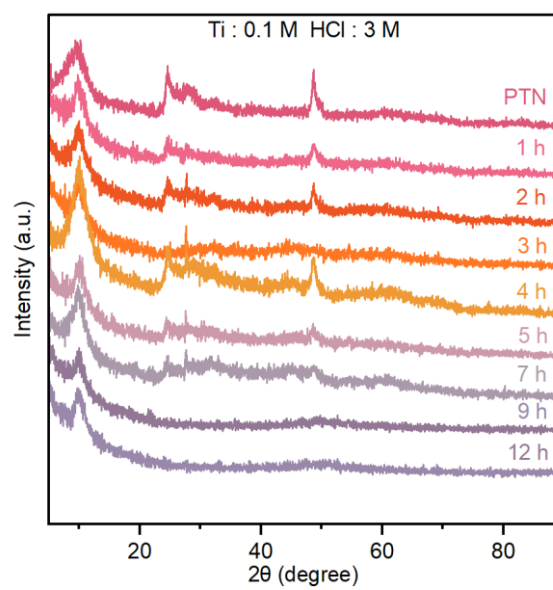


Figure S12. pXRD patterns of undissolved PTN sampled after different durations of mixing PTN with acid. Reaction condition: 0.1 M Ti in 3 M HCl.

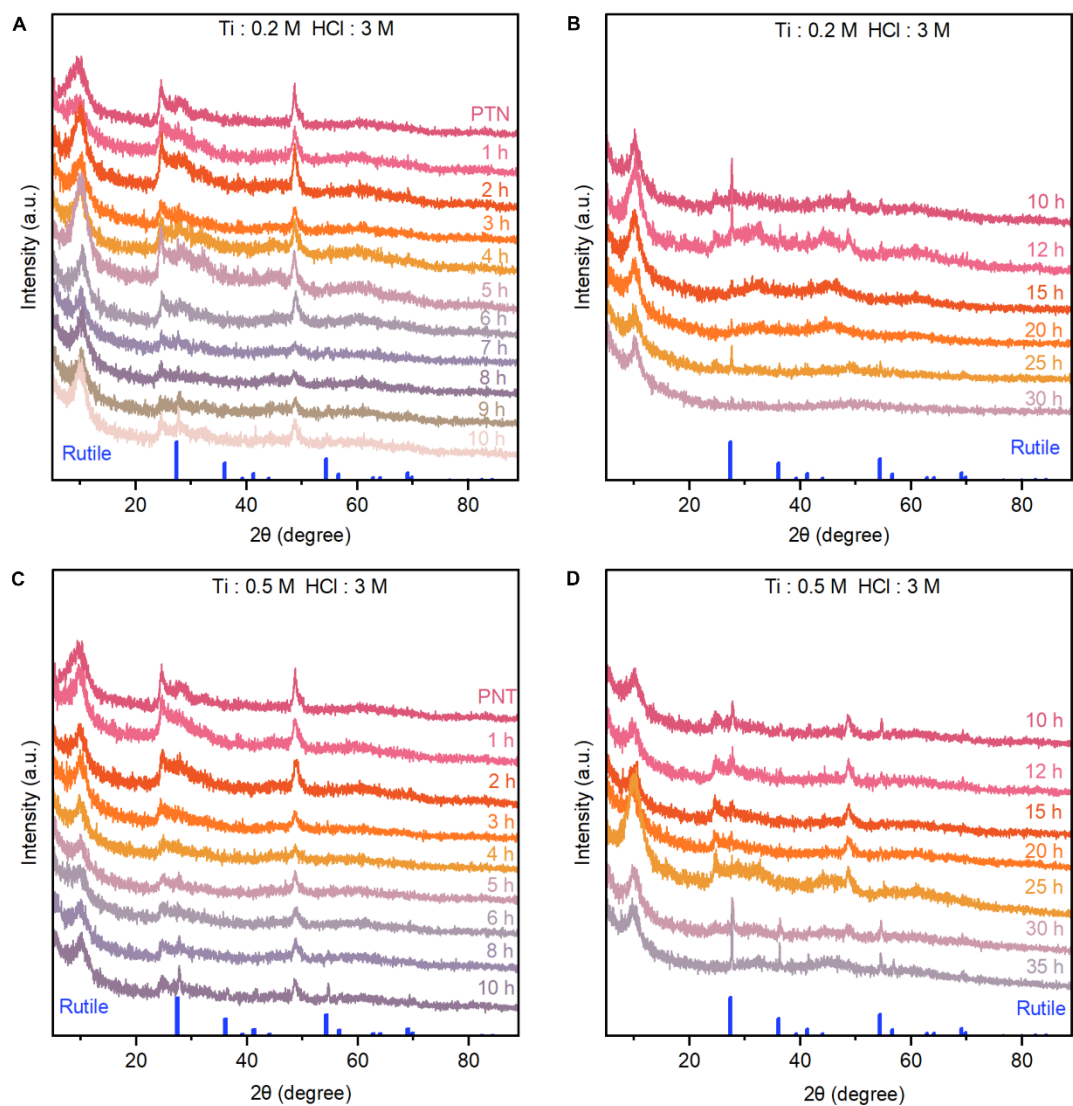


Figure S13. pXRD patterns of undissolved PTN sampled after different durations of mixing PTN with acid. Reaction condition: (A, B) 0.2 M Ti in 3 M HCl, and (C, D) 0.5 M Ti in 3 M HCl.

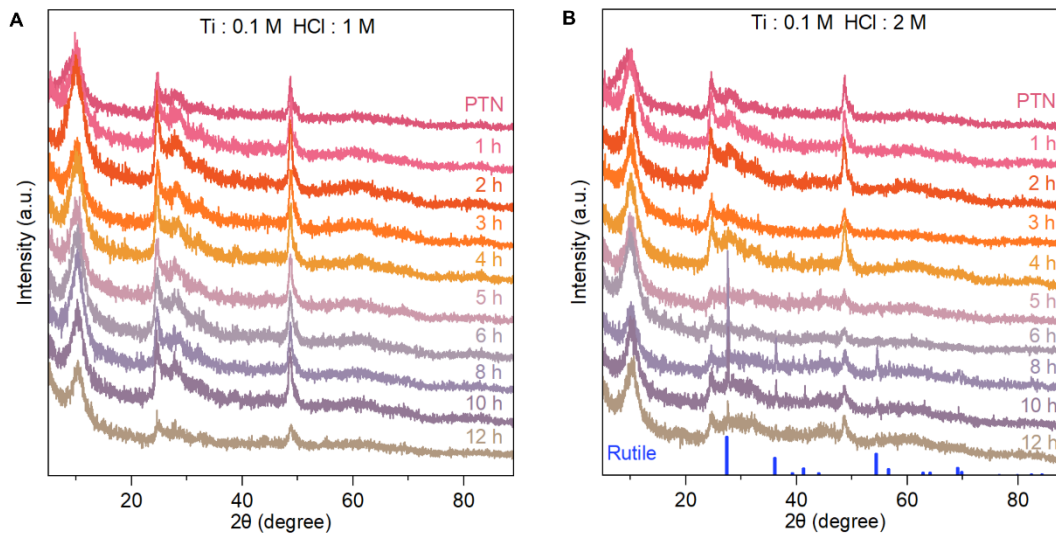


Figure S14. pXRD patterns of undissolved PTN sampled after different durations of mixing PTN with acid. Reaction condition: (A) 0.1 M Ti in 1 M HCl, and (B) 0.1 M Ti in 2 M HCl.

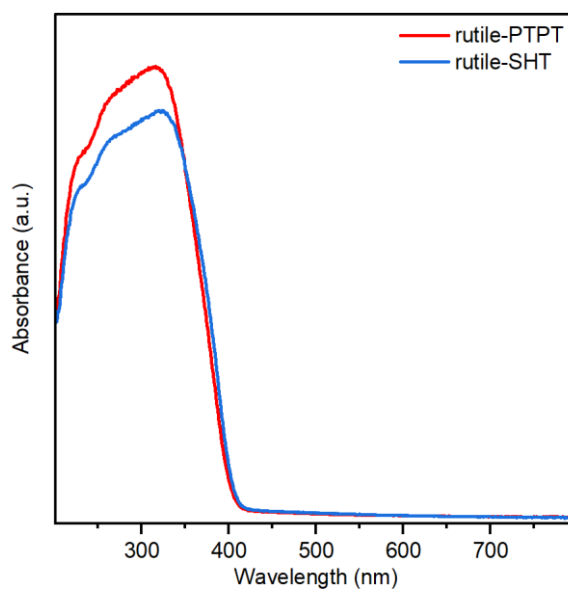


Figure S15. UV-Vis diffuse reflection spectroscopy of the rutile products collected from the hydrothermal treated clear solution (rutile-SHT) and PTN (rutile-PTPT).

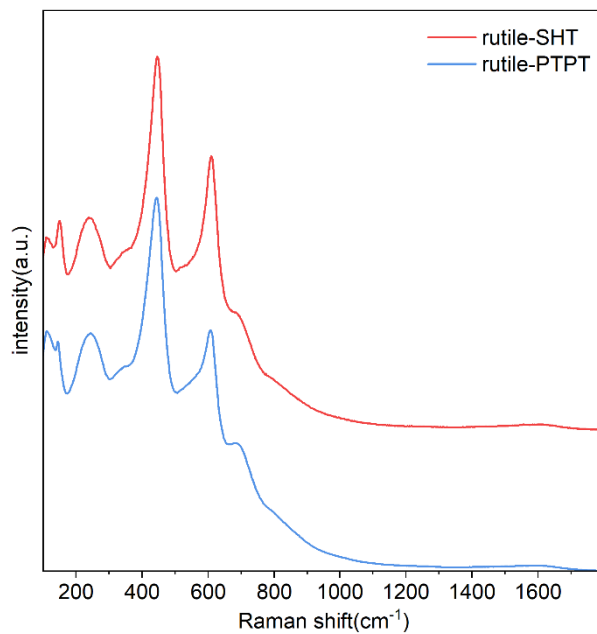


Figure S16. Raman spectra of the rutile-SHT and rutile-PTPT.

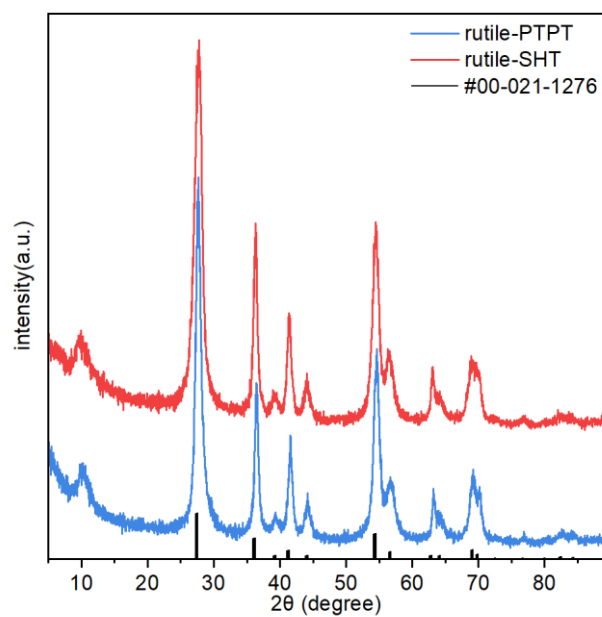


Figure S17. pXRD patterns of the rutile-SHT and rutile-PTPT (0.5 M Ti concentration).

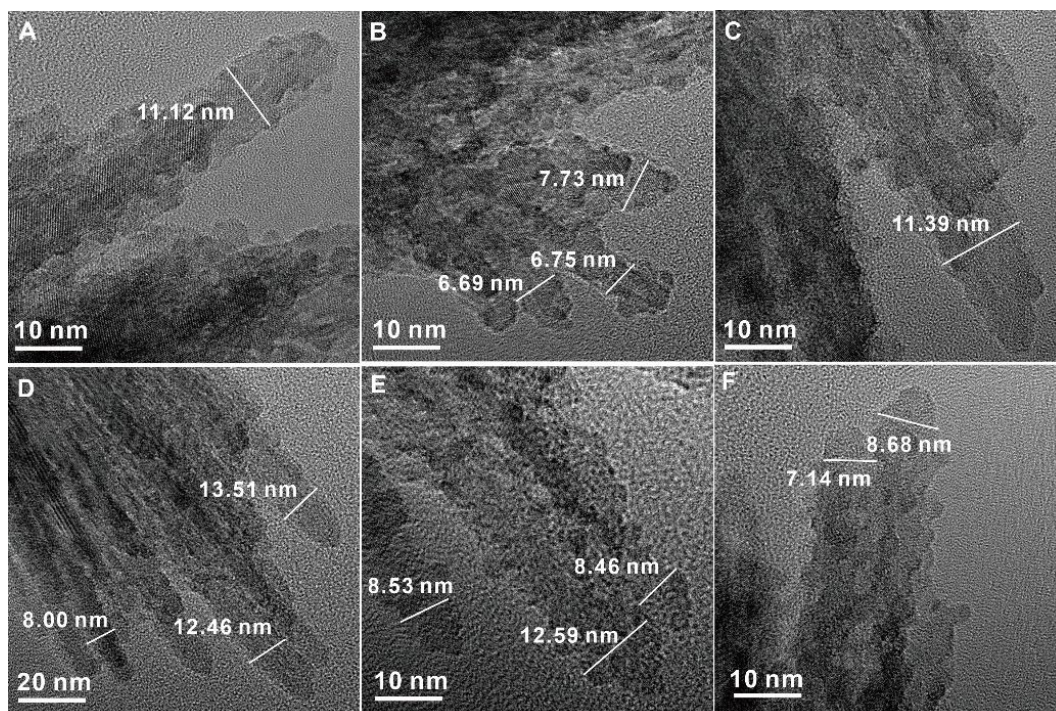


Figure S18. Representative TEM images of rutile-SHT.

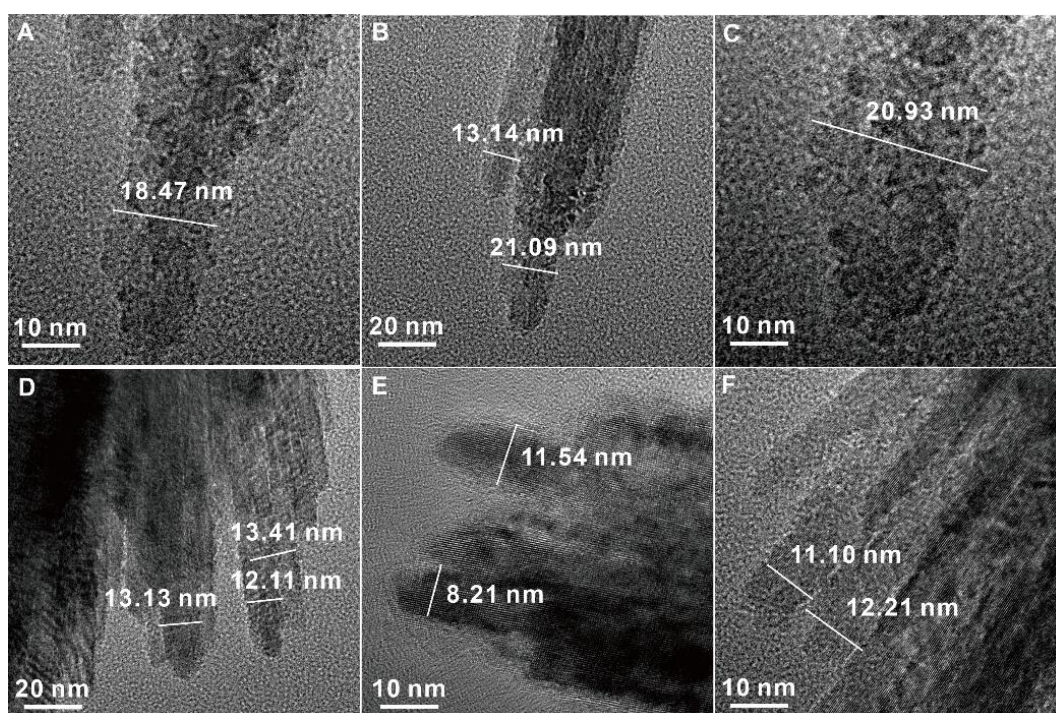


Figure S19. Representative TEM images of rutile-PTPT.

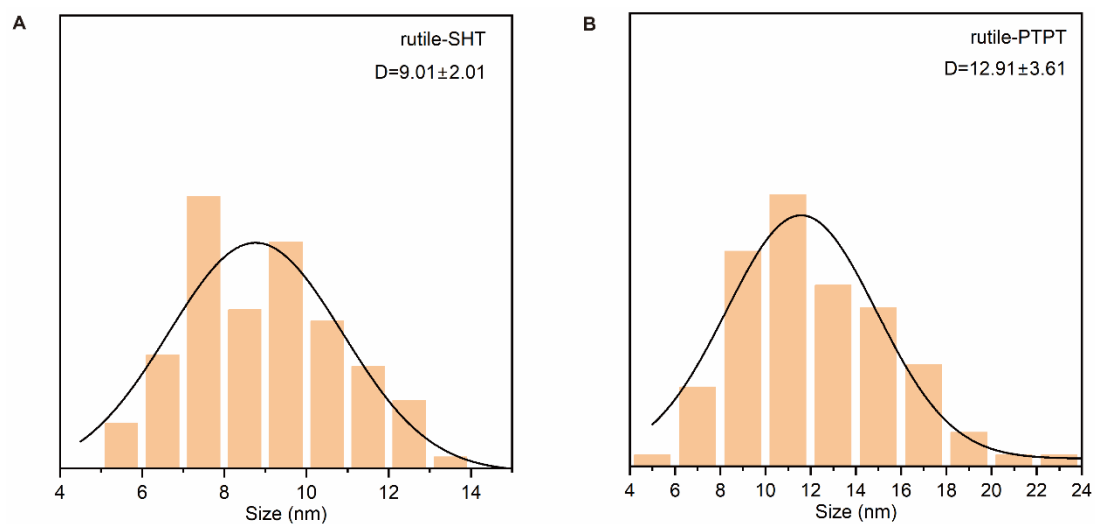


Figure S20. Statistics on the diameter size distributions (based on TEM images) of rutile products gained from two different reaction conditions.

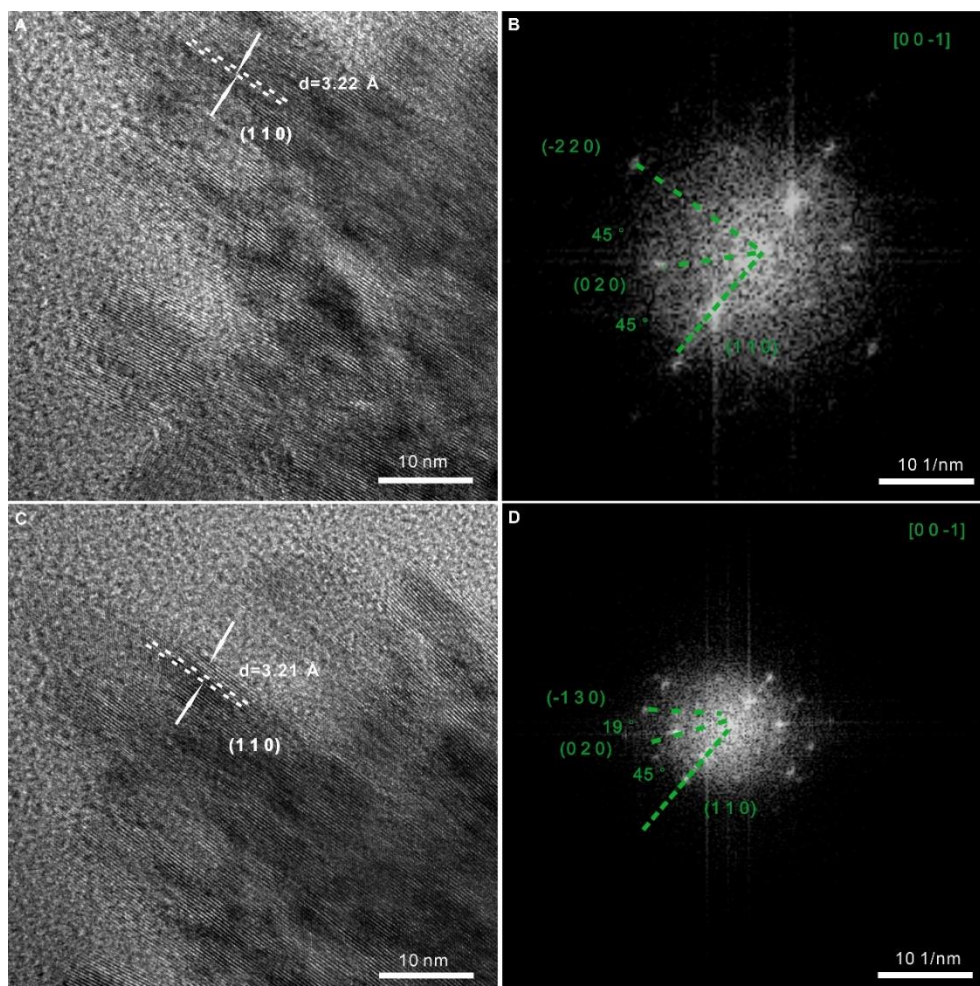


Figure S21. Representative HRTEM images and the fast Fourier-transformation (FFT) results of rutile-SHT.

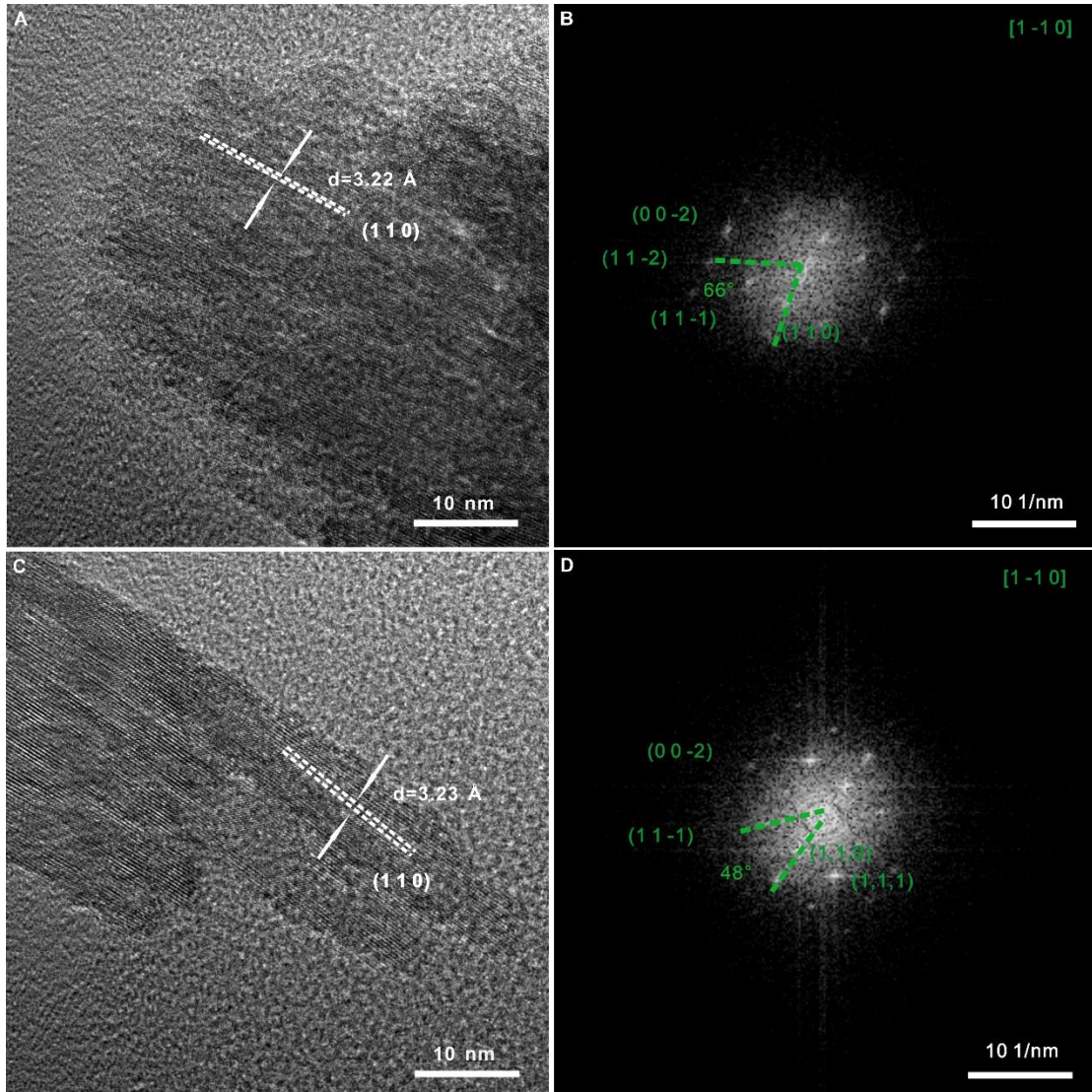


Figure S22. Representative HRTEM images and the fast Fourier-transformation (FFT) results of rutile-PTPT.

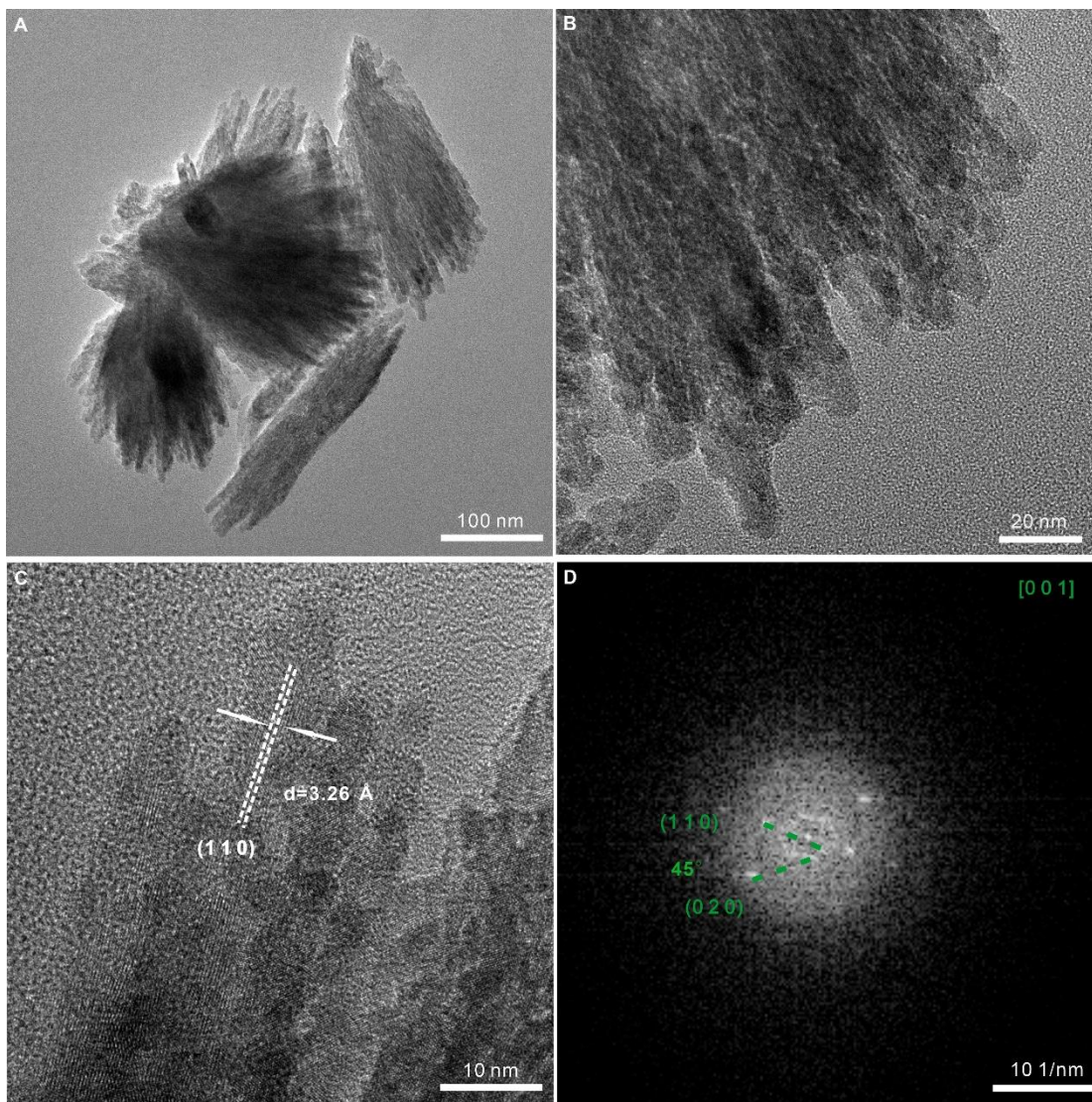


Figure S23. Representative TEM and HRTEM images, and the fast Fourier-transformation (FFT) results of rutile-SHT (0.5 M Ti concentration).

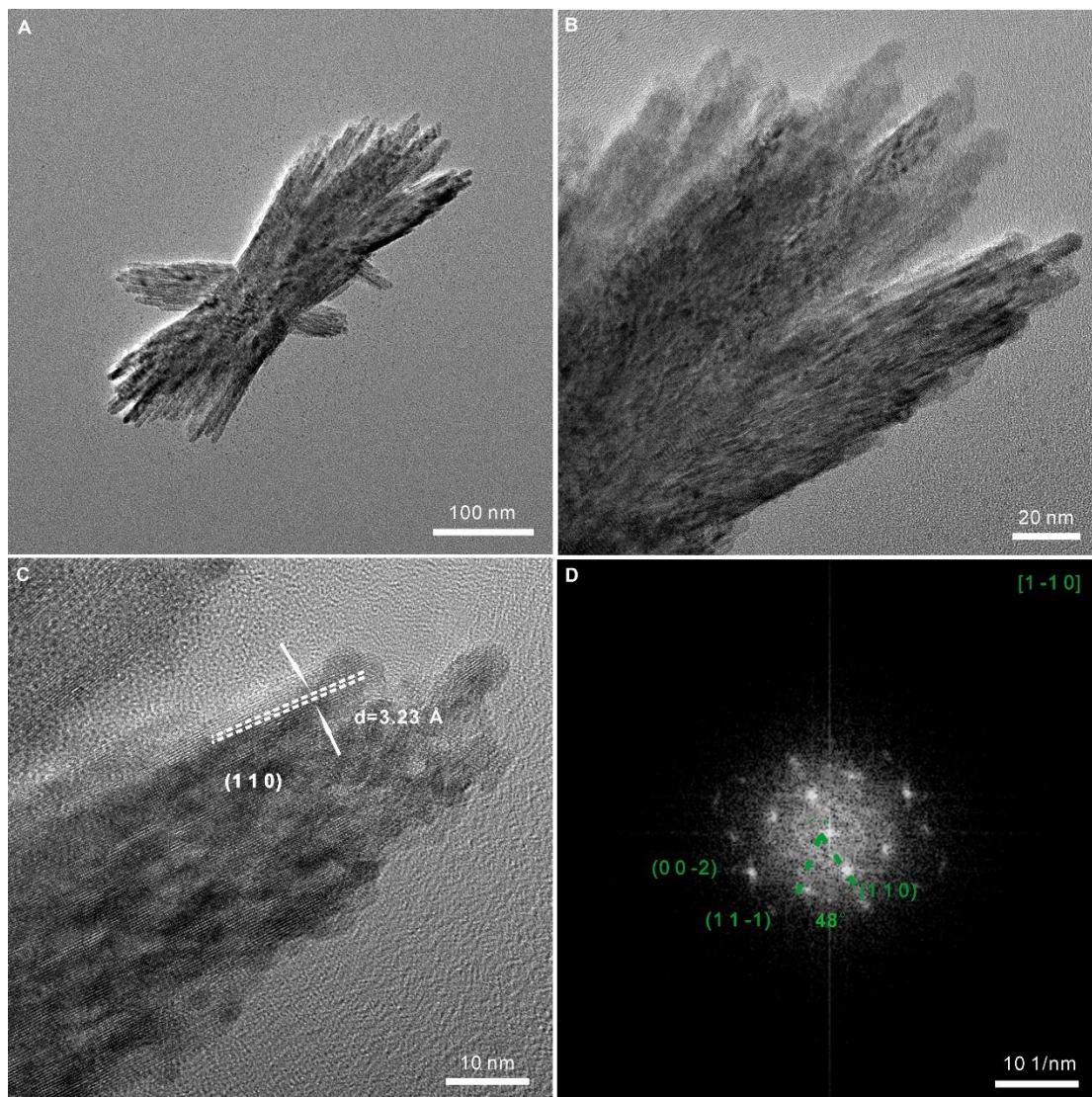


Figure S24. Representative TEM and HRTEM images, and the fast Fourier-transformation (FFT) results of rutile-PTPT (0.5 M Ti concentration).

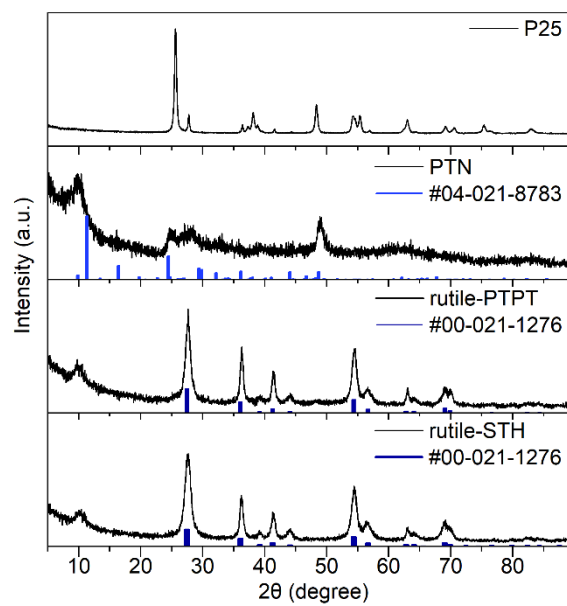


Figure S25. pXRD patterns of P25, PTN synthesized by P25, rutile-PTPT and rutile-STH.

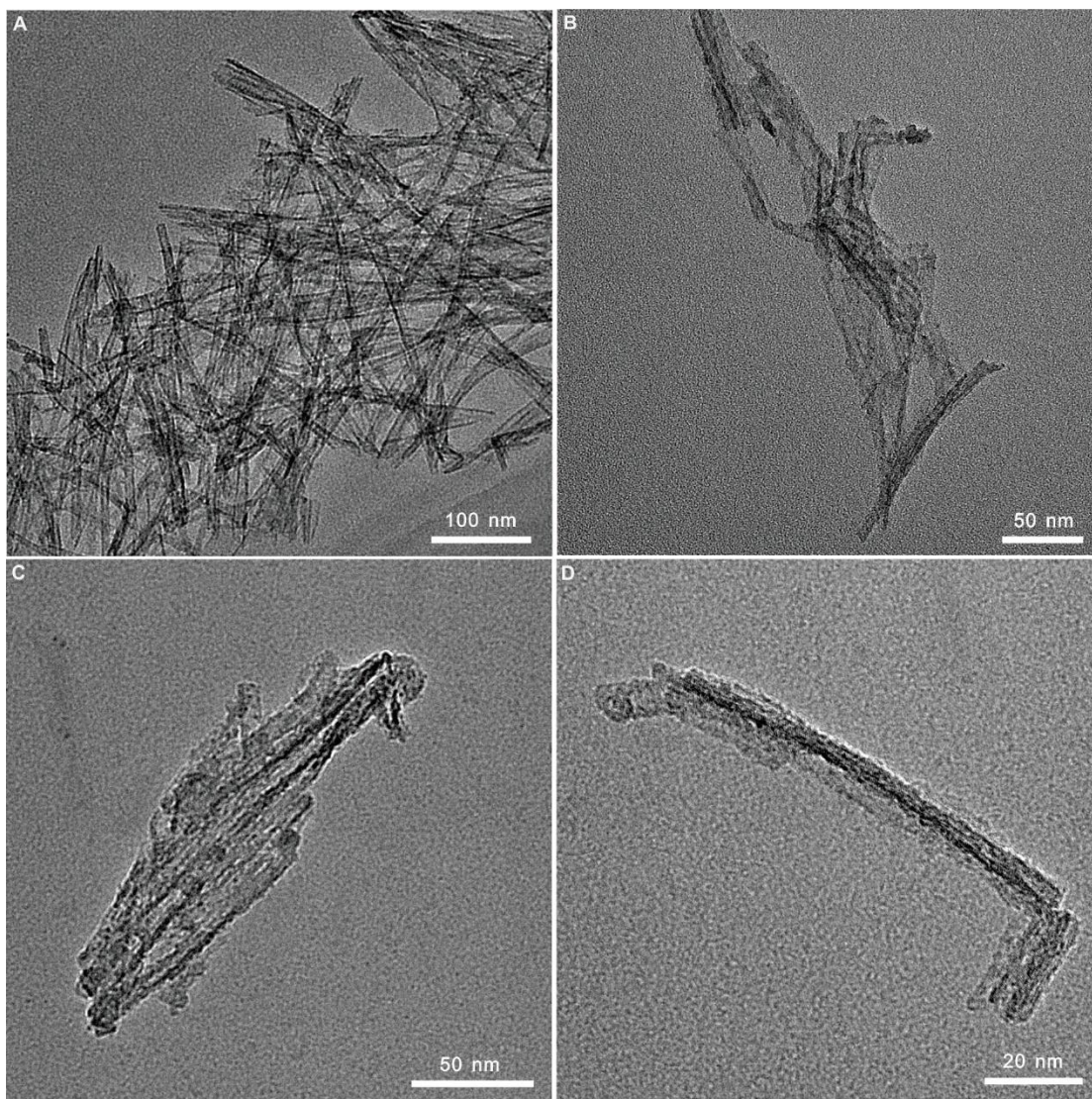


Figure S26. Representative TEM image (A-C) and HRTEM images (D) of PTN synthesized from P25.

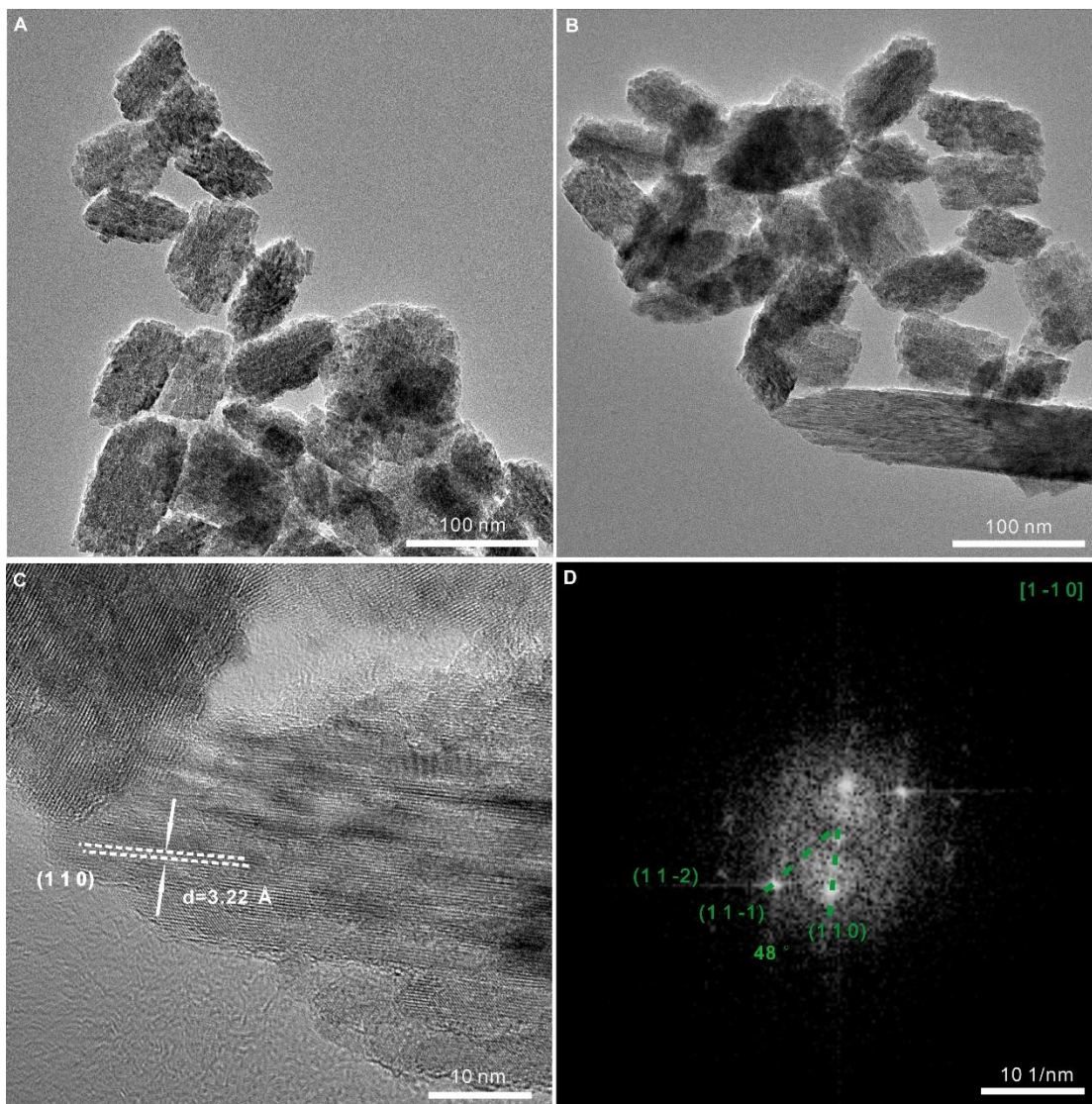


Figure S27. Representative TEM image (A) and HRTEM image (B-C, D is FFT) of rutile-PTPT synthesized from P25.

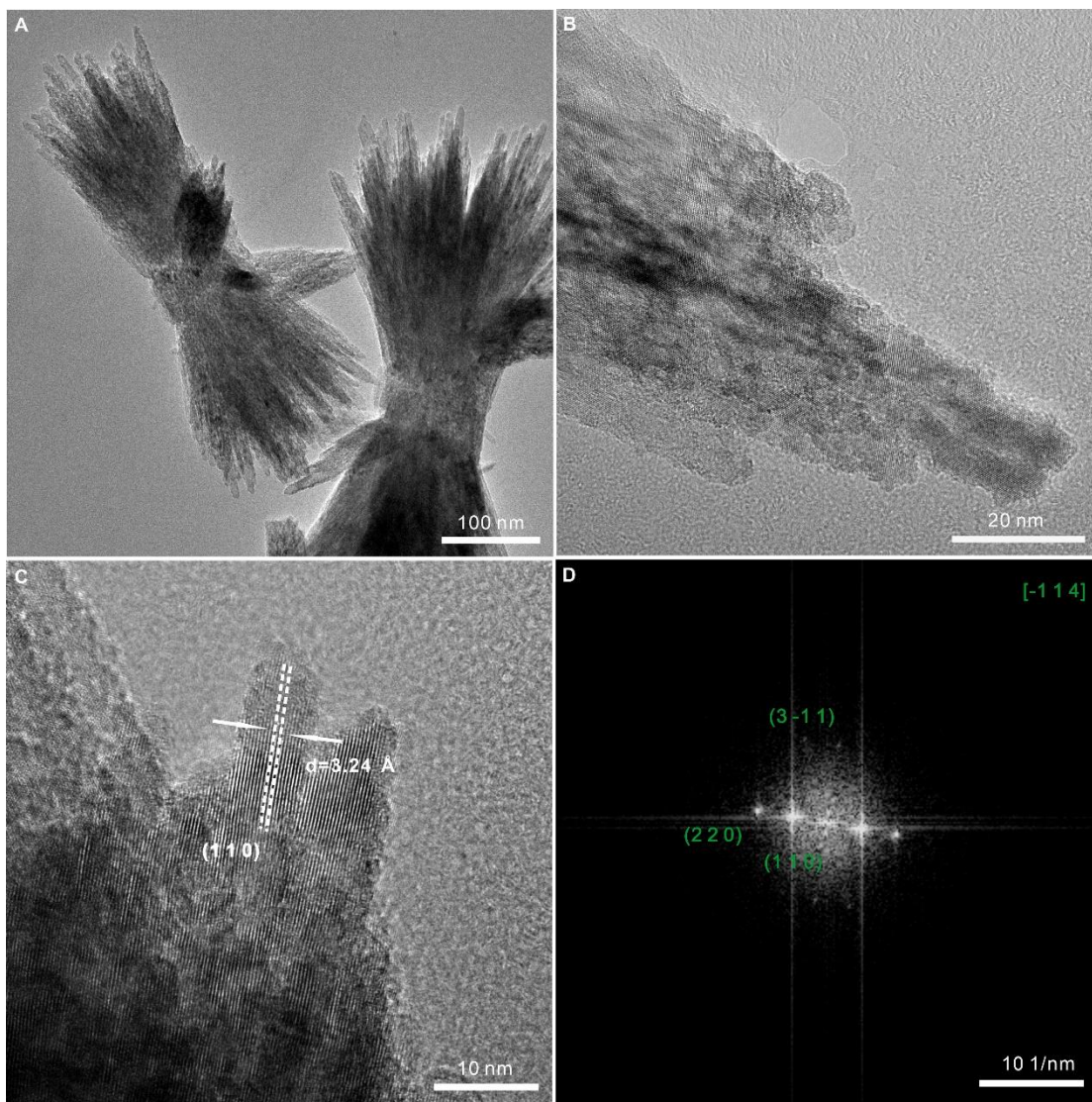


Figure S28. Representative TEM image (A) and HRTEM image (B-C, D is FFT) of rutile-SHT synthesized from P25.

Table S1. Band gaps of undissolved PTN sampled after different times of mixing PTN with acid.

Stir time (h)	Band gap (eV)
0	3.35
1	3.28
2	3.25
3	3.31
4	3.30
5	3.31
7	3.32
9	3.32
12	3.31

REFERENCES

1. Zhu, H. Y.; Lan, Y.; Gao, X. P.; Ringer, S. P.; Zheng, Z. F.; Song, D. Y.; Zhao, J. C., Phase Transition between Nanostructures of Titanate and Titanium Dioxides via Simple Wet-Chemical Reactions. *J. Am. Chem. Soc.* **2005**, *127* (18), 6730-6736.